EXAMINATION OF IRRADIATED V-4Cr-4Ti PRESSURIZED CREEP TUBES - D. S. Gelles*, K. Fukumoto (Graduate School of Nuclear Power and Energy Safety Engineering, University of Fukui, Fukui 910-8507, Japan), T. Muroga (National Institute for Fusion Science, Oroshi, Toki, Gifu 509-5292, Japan) and R. J. Kurtz* (Pacific Northwest National Laboratory)*

OBJECTIVE

The objective of this effort is to quantify microstructural response in irradiated V-4Cr-4Ti pressurized tubes in order to better understand irradiation creep mechanisms.

SUMMARY

US and Japanese pressurized tubes of V-4Cr-4Ti contained in the HFIR 17J irradiation experiment at 600°C to 3.7 dpa have been examined by transmission electron microscopy. Analysis was intended to determine Burgers vector anisotropy in order to provide understanding of dislocation development resulting from irradiation creep. Both materials were found to have developed precipitation in reactor at 600ºC, the US heat probably containing TiO_2 and the Japanese heat forming oxy-carbo-nitrides, but precipitation did not prevent satisfactory dislocation imaging. Also, it was found that V-4Cr-4Ti develops both $\frac{a}{2}$<111> and a<100> Burgers vectors during irradiation, with the a<100> dislocation densities similar to those with $\frac{a}{2}$<111> for an unstressed condition but lower as a result of applied stress. However, Burgers vector anisotropy measurements in V-4Cr-4Ti did not show the large variations found in ferritic steels.

PROGRESS AND STATUS

Introduction

It is now well understood that irradiation creep for practical applications is a consequence of radiation induced dislocation loop nucleation, growth, intersection with matrix dislocations, and evolution into dislocation networks due to an applied stress. It is also well established that both dislocation nucleation and climb (or motion) are affected by the applied stress called Stress Induced Preferential Nucleation (SIPN) and Stress Induced Preferential Absorption (SIPA) so that certain Burgers vectors are favored. This results in what can be termed Burgers vector anisotropy, and when deformation is entirely due to dislocation evolution, the induced creep strain is simply a measure of the anisotropy in dislocation motion so that

$$\dot{\epsilon} = \sum_i \rho_i \bar{b}_i \bar{v}_i \qquad (1)$$

where $\dot{\epsilon}$ is the plastic strain rate, i defines each of the possible Burgers vectors, $\bar{b}$, ρ is the dislocation density and $\bar{v}_i$ is the average dislocation velocity for each Burgers vector [1]. Therefore, as irradiation induced deformation proceeds under stress, dislocations with Burgers vectors optimally oriented will develop enhanced densities and as point defects are absorbed, they will move at least as far as unfavorably oriented Burgers vectors, resulting in a net change in shape. However, it can be noted that once an anisotropy is established by an imposed stress state, then that anisotropy will continue to increase unless a mechanism is imposed to stabilize the anisotropy.

The present effort is intended to quantify this Burgers vector anisotropy. Burgers vector anisotropy is difficult to quantify because a procedure is required that is able to identify all Burgers vectors in a field of view. In fact, procedures have now been developed to identify all Burgers in austenitic [2,3] and ferritic steels [4]. However, in both cases, the analysis is complicated by development of two types of Burgers vectors. For example, austenitic steels develop Frank loops as well as perfect dislocations, and ferritic steels are found to develop a<100> Burgers vectors during irradiation along with the usual $\frac{a}{2}$<111>. It was anticipated that

* Pacific Northwest National Laboratory (PNNL) is operated for the U.S. Department of Energy by Battelle Memorial Institute under contract DE-AC06-76RLO-1830.

vanadium alloys would have the advantage that only one Burgers vector would be present, of the type $\frac{a}{2}$<111>, and therefore only four variants had to be examined. In a previous report, pressurized tubes of V-4Cr-4Ti were examined following irradiation at 425°C, but it was found to be impossible to identify dislocation structures in those conditions due to heavy precipitation of oxy-carbo-nitrides [5]. The present effort instead examines conditions irradiated at 600°C where the effects of precipitation are not expected.

The present effort has the added advantage that two heats of V-4Cr-4Ti were irradiated side by side in the HFIR 17J test, the US heat 832665 and the Japanese heat NIFS-heat2. These heats differ primarily in impurity levels, with the US heat having higher oxygen and the Japanese heat with higher nitrogen. The present experiment therefore consists of examinations of six conditions: zero, intermediate and high stress levels for each of the heats. A condition that had failed was also examined. Results of diameter change following irradiation for the Japanese tubes have been reported [6] and the behavior of the US tubes has been analyzed [7].

Experimental Procedure

The results of diameter change measurements for V-4Cr-4Ti pressurized tubes from the HFIR 17J test have been kindly provided by Meimei Li and are listed in Table 1 [7]. Those specimens selected for destructive examination are marked with a star, but selection of UN02 was made before creep strain information had been obtained. As noted in the table, specimen UN02 was found to contain a residue believed to be a lithium compound and indicating that the low strain value was due to leakage. Therefore, specimens UN05 and UN12 also probably leaked, and UB-19 is confirmed to have leaked [7]. Furthermore, as diameter change is expected to be linear with time and the strain for UN02 is approximately 27% for that of UN17, it is expected that UN02 failure occurred after about a quarter of the irradiation cycle, and most likely as a result of a weld failure. Detailed information on specimen preparation has been reported previously [3,4], but in summary, tubes were sectioned and then punched using a curved mandrell producing curved disks which were then electopolished in a Tenupol polishing apparatus with a solution of 10% sulfuric acid in methanol at dry ice temperature. Microscopy was performed using a JEOL 2010 transmission electron microscope operating at 200 KeV and images were recorded digitally and processed using Photoshop. The orientation of the disk curvature in the microscope was set so that the longitudinal direction of the tube corresponded to the x-tilt axis and therefore the stress state was known. Tilt conditions were recorded for each image. Stereo measurements were used to determine specimen thickness and a line intersection method was used to determine dislocation density for each Burgers vector of interest.

Table 1. Test conditions for specimens of interest irradiated in the 17J test at 600ºC to 3.7 dpa [7].

Tube ID	Heat	Midwall Effective Stress (MPa)	Effective mid-wall strain (%)	Comments
UB00*	US heat: 832665	0.5	0.004	
UB15	US heat: 832665	29.6	0.054	
UB08	US heat: 832665	57.4	0.109	
UB03	US heat: 832665	127.2	0.266	
UB12*	US heat: 832665	113.1	0.221	
UB06*	US heat: 832665	166.8	0.503	
UB19	US heat: 832665	165.2	0.012	leak
UN19*	NIFS-Heat2	0.5	0.011	
UN08	NIFS-Heat2	30	0.118	
UN13*	NIFS-Heat2	58.7	0.286	
UN05	NIFS-Heat2	115.6	0.026	
UN12	NIFS-Heat2	114.4	0.104	
UN02*	NIFS-Heat2	172.5	0.330	Contained lithium
UN17*	NIFS-Heat2	172.5	1.228	

* Specimen sectioned for examination.

The procedure used to identify Burgers vectors matched that used previously [5], requiring six images of the same area and involving tilts of approximately 45°. An image using $\bar{g}$=<200> is expected to show all of the $\frac{a}{2}$<111> dislocations present, whereas any $\bar{g}$=<110> such as [01$\bar{1}$] should only show two of the four possibilities and allow separation of the dislocation populations into two groups of two Burgers vectors. A second $\bar{g}$=<110> such as [$\bar{1}$10] will in fact allow separation of each of these groups. However, comparison of images to unambiguously identify those dislocations that appear is very difficult given the large tilts between images and therefore the procedure uses stereo imaging, and two images separated by about 10° of tilt are needed for each $\bar{g}$ used. However, only images approaching weak beam conditions proved satisfactory for $\bar{g}$=<200> in thicker specimens, and those images have been inverted for analysis.

Stereo images are presented as anaglyphs, requiring the standard red-blue or red-green glasses for viewing. In order to maximize the depth of the stereo for a given anaglyph, the image must be rotated so that the operating $\bar{g}$, indicated by an arrow, appears vertical. All micrographs contain a 200 nm magnification marker appearing as a white bar.

Results

Examinations revealed differences between the US and Japanese heats. No voids were observed but both were found to contain uniform distributions of precipitates following irradiation at 600°C, but precipitate densities were much lower than those observed following irradiation at 425°C [5], and precipitation did not appear to affect the dislocation structures. Examples are provided in Figure 1, showing the US heat in (a) and the Japanese heat in (b), both imaged using $\bar{g}$=<110> near (001). The US heat contains small circular platelets ~40 nm in diameter on {100} planes, with two orientations showing in this image, one approximately vertical and the other approximately horizontal, both viewed on edge, and the Japanese heat shows a similar density of smaller equiaxed precipitates ~10 nm in diameter. Therefore, precipitation response was different for the two materials.

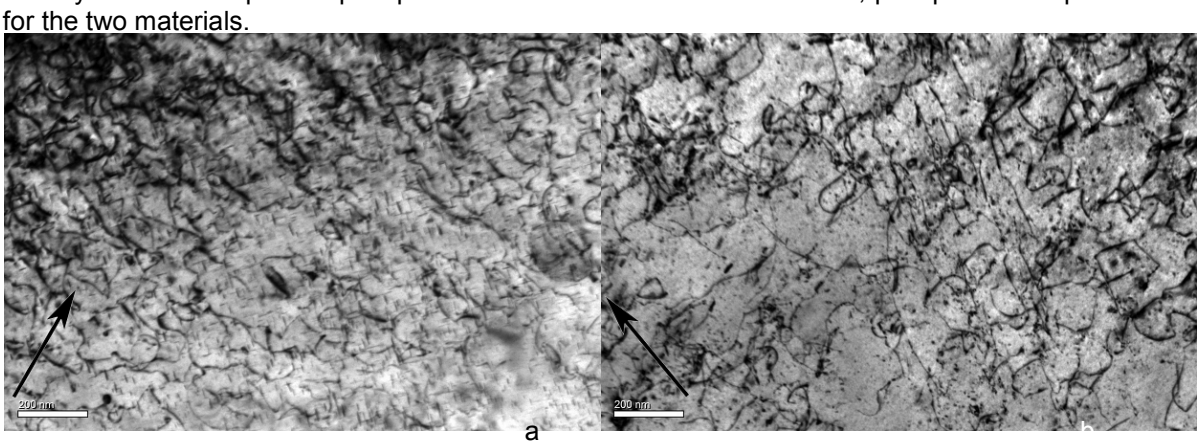

Figure 1. Dislocations and precipitation in pressurized tubes UB06 (a) and UN17 (b) irradiated at 600ºC to dpa at midwall effective stress levels of ~170 MPa.

Examination of images revealed a problem with the starting assumptions for this project. It was assumed that all Burgers vectors would be of type $\frac{a}{2}$<111> but comparison of images raised questions with that assumption. If all Burgers vectors were of type $\frac{a}{2}$<111>, then all dislocations would be visible in $\bar{g}$=<200> contrast. Figure 2 provides comparison of images using $\bar{g}$=[01$\bar{1}$], $\bar{g}$=[200], and $\bar{g}$=[$\bar{1}$10], respectively, for specimen UN19, the unstressed Japanese tube. Careful examination reveals images, particularly in $\bar{g}$=[$\bar{1}$10] contrast but also in $\bar{g}$=[01$\bar{1}$] contrast that do not appear in $\bar{g}$=[200] contrast. They tend to be straight dislocation segments, whereas most of the dislocations in $\bar{g}$=[200] contrast appear as loops or arcs. As no stacking faults are apparent, and examples will be shown where variations in intensity occur for different dislocation segments, it is anticipated that a<100> Burgers vectors have been produced during irradiation in V-4Cr-4Ti. Fortunately, the problem of determining Burger's vector anisotropy for ferritic steels has been developed [4]. For that

case, where both $\frac{a}{2}$<111> and a<100> exist, the procedure uses the same images as were collected for this study, but the analysis is more complex.

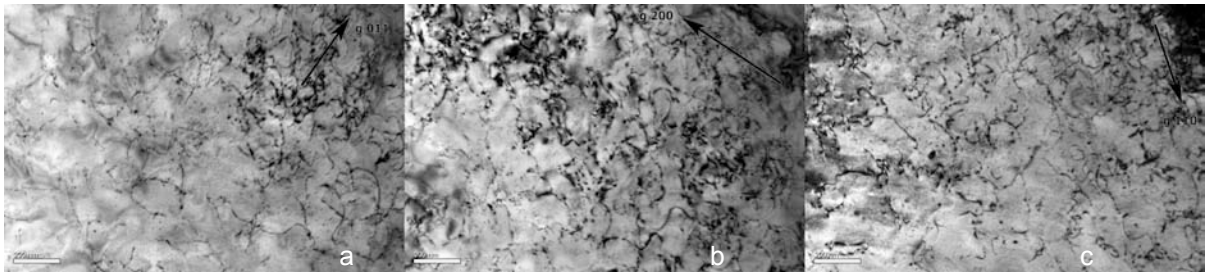

Figure 2. Comparison of images for $\bar{g}$=[01$\bar{1}$] in (a), $\bar{g}$=[200] in (b), and $\bar{g}$=[$\bar{1}$10] in (c) for condition UN19, an unstressed tube of the Japanese heat of V-4Cr-4Ti.

The dislocation structures as stereo pairs for the conditions examined are shown in Figures 3 through 9. However, in order to optimize resolution, these images have been rotated (counterclockwise) with respect to all other images in this report so that the longitudinal direction of the tube is now towards one o'clock. In each case, the $\bar{g}$=<200> image is in the center (b) and the corresponding $\bar{g}$=<110> images are on either side at (a) and (c). Each image contains an arrow indicating the direction for $\bar{g}$, so that to maximize the stereo effect, the viewer should rotate the image so the arrow points away. However, note that to invert the top and bottom of the stereo image, one need only rotate the picture 180º. The stress axis can be envisioned as follows: the length of the tube is in approximately the vertical direction but actually rotated ~25º clockwise or towards one o'clock as shown inset, the radial tube direction is orthogonal, and the tube thickness is in the direction of the stereo effect (ideally with the sample at zero tilt).

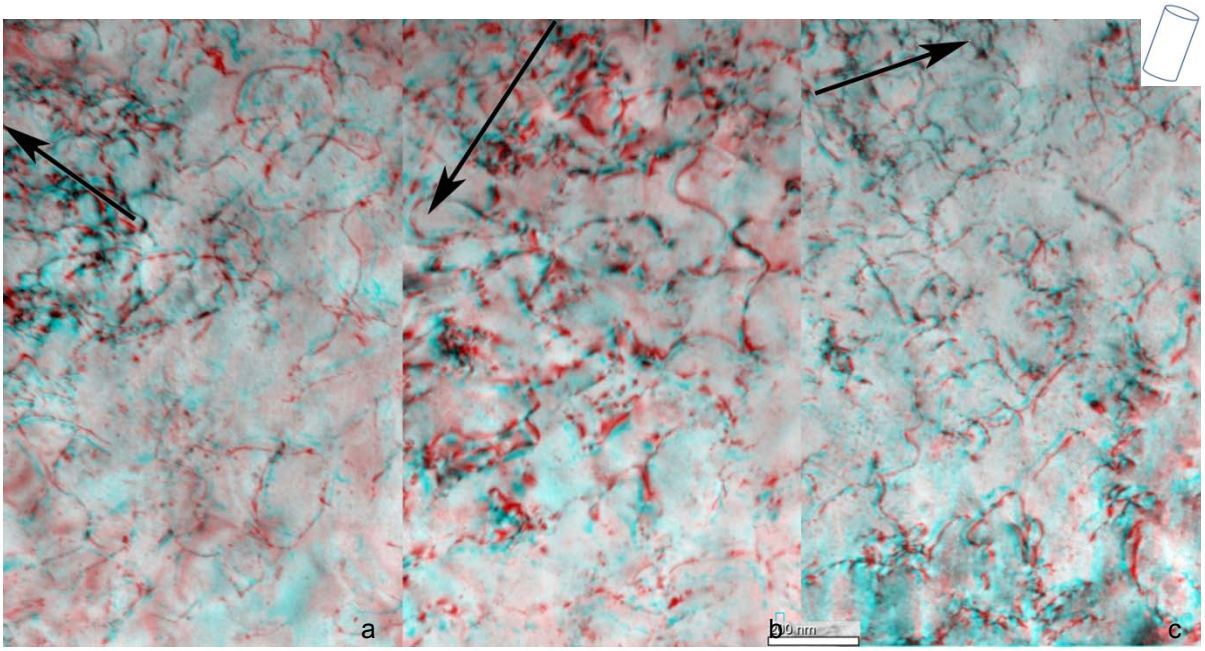

Figure 3. Anaglyph stereo images of dislocation structure in Japanese heat specimen UN19 unstressed with $\bar{g}$=[01$\bar{1}$] contrast in (a), $\bar{g}$=[200] contrast in (b) and $\bar{g}$=[$\bar{1}$10] contrast in (c).

It should first be noted that the images for Figures 7, 8 and 9 are for much thicker samples than those for Figures 3, 4, 5 and 6. This is a result of examining the US specimens first, and not yet understanding how difficult it would be to analyze such images for Burgers vector anisotropy. For example, thicker samples required weak beam dark field imaging to successfully see all dislocations in <200> contrast, whereas for thinner samples, bright field imaging was adequate.

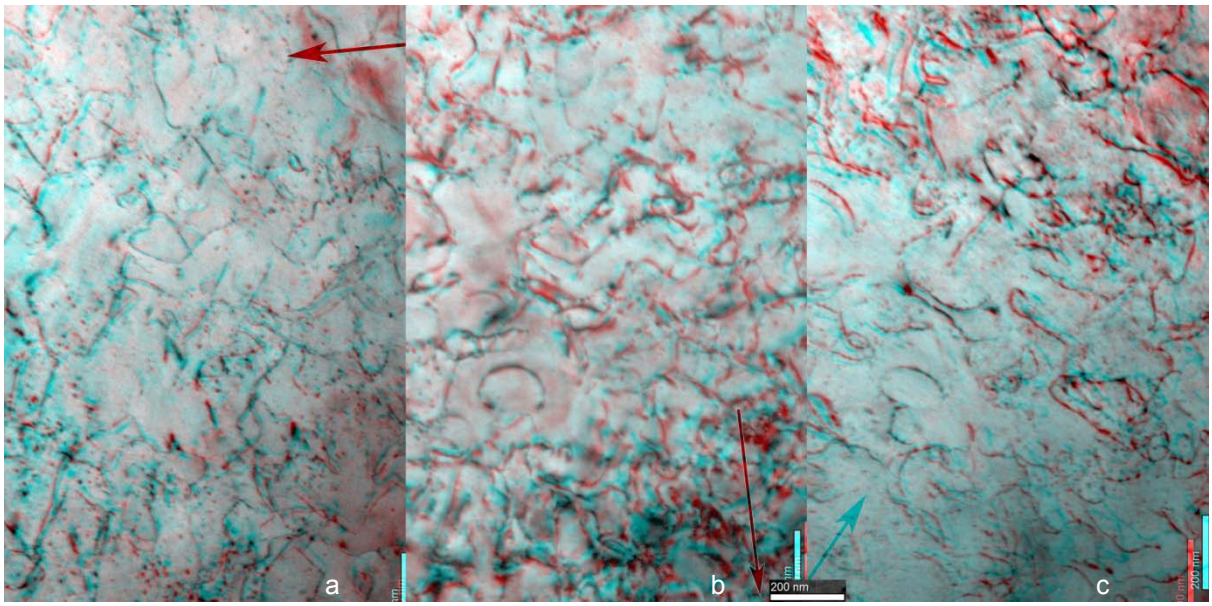

Figure 4. Anaglyph stereo images of dislocation structure in specimen UN13 at 58.7 MPa with $\bar{g}$=[01$\bar{1}$] contrast in (a), $\bar{g}$=[200] contrast in (b) and $\bar{g}$=[$\bar{1}$10] contast in (c).

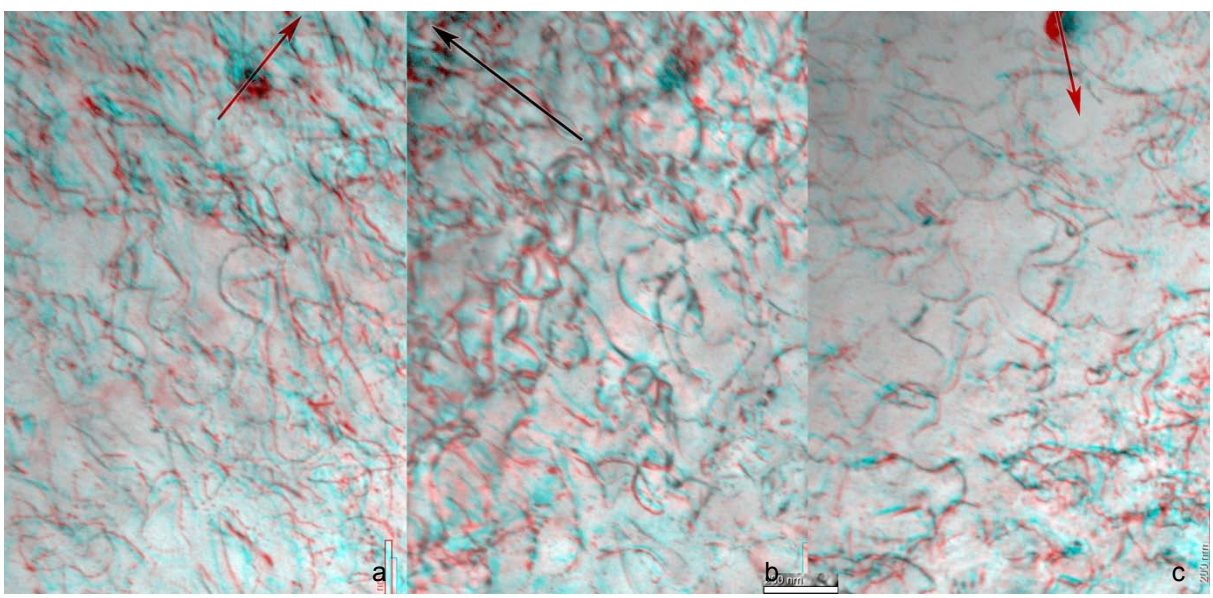

Figure 5. Anaglyph stereo images of dislocation structure in specimen UN17 at 172.5 MPa with $\bar{g}$=[01$\bar{1}$] contrast in (a), $\bar{g}$=[200] contrast in (b) and $\bar{g}$=[$\bar{1}$10] contrast in (c).

Therefore, the images for the Japanese tube conditions were analyzed first. The procedure can be best envisioned based on Figure 10 showing three of the six imaging conditions used; $\bar{g}$=[01$\bar{1}$], $\bar{g}$=[200] and $\bar{g}$=[$\bar{1}$10]. A truth table defining dislocation contrast conditions for the various possible imaging conditions is given in Table 2. (The $\bar{g}$=[$\bar{1}$01] imaging condition is included, but happens not to apply to any of the imaging sequences used in this study.) From Table 2, it can be determined that for [200] imaging, all $\frac{a}{2}$<111> as well as a[100] Burgers vectors should be visible. For $\bar{g}$=[01$\bar{1}$] imaging, only half the $\frac{a}{2}$<111> as well as a[010] and a[001] Burgers vectors should be visible. Therefore, the $\bar{g}$=[01$\bar{1}$] and $\bar{g}$=[200] images can be compared to

identify those which appear only in $\bar{g}=[01\bar{1}]$ contrast, only in $\bar{g}=[200]$ contrast or both, to separate the dislocations into three groups. Likewise, the $\bar{g}=[200]$ and $\bar{g}=[\bar{1}10]$ images can be compared to separate the dislocations into three somewhat different groups. Then, comparison of these groups can uniquely determine which Burgers vector corresponds to each dislocation image.

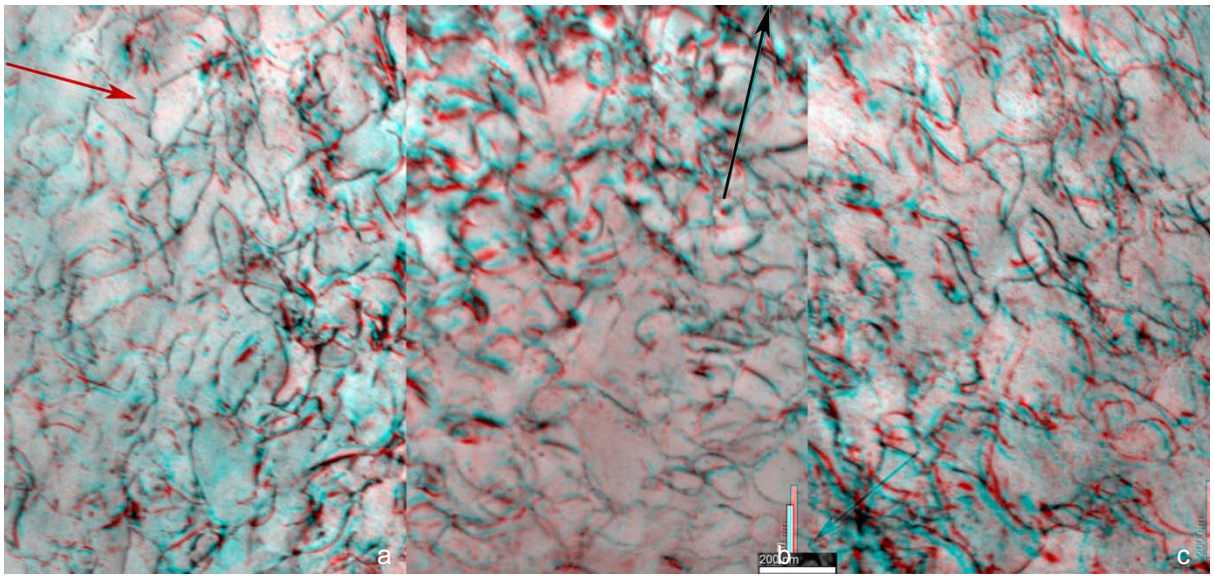

Figure 6. Anaglyph stereo images of dislocation structure in specimen UN02 at 172.5 MPa but believed to have failed at ~25% of the strain of specimen UN17 with $\bar{g}=[01\bar{1}]$ contrast in (a), $\bar{g}=[200]$ contrast in (b) and $\bar{g}=[\bar{1}10]$ contrast in (c).

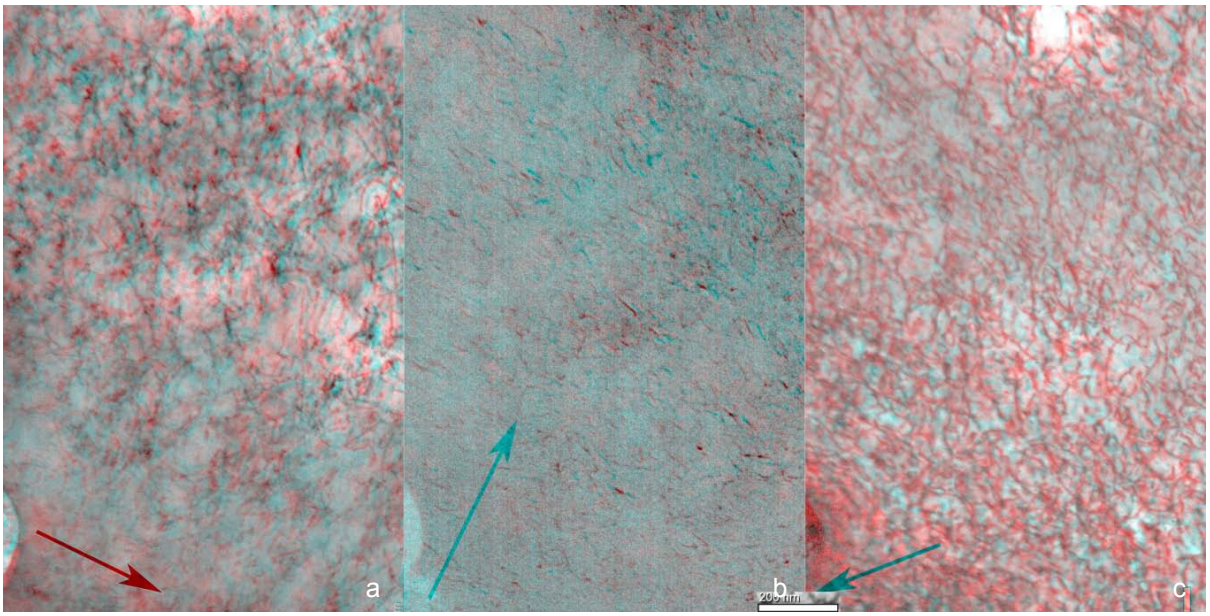

Figure 7. Anaglyph stereo images of dislocation structure in US heat specimen UB00 unstressed with $\bar{g}=[01\bar{1}]$ contrast in (a), $\bar{g}=[200]$ contrast in (b) and $\bar{g}=[\bar{1}10]$ contrast in (c).

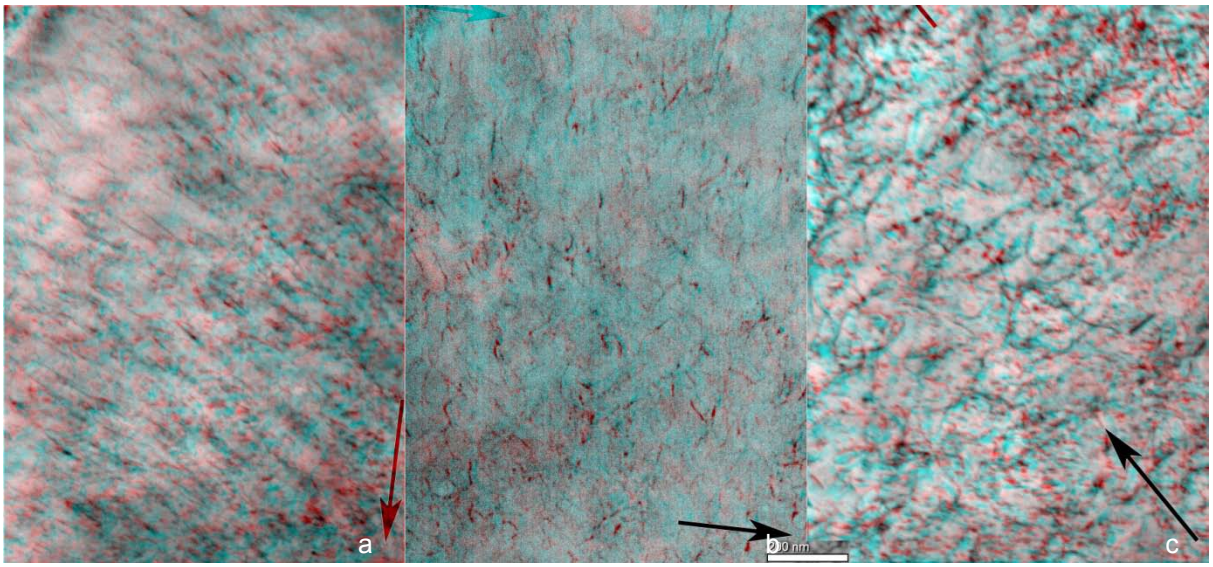

Figure 8. Anaglyph stereo images of dislocation structure in specimen UB12 at 113.1 MPa with $\bar{g}=[01\bar{1}]$ contrast in (a), $\bar{g}=[200]$ contrast in (b) and $\bar{g}=[\bar{1}10]$ contrast in (c).

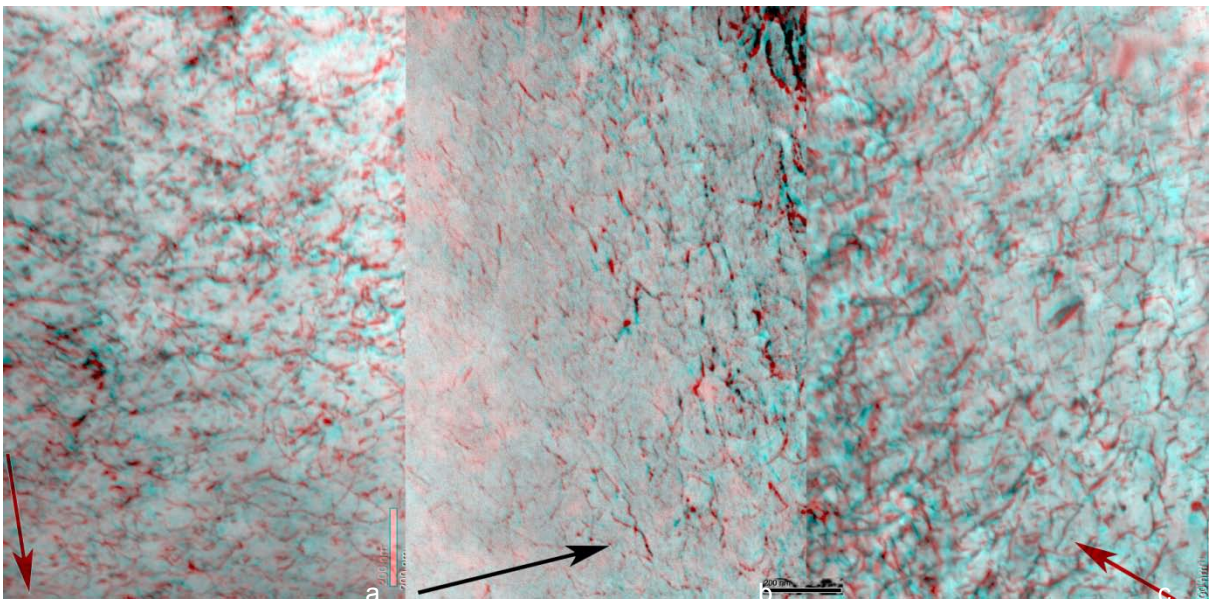

Figure 9. Anaglyph stereo images of dislocation structure in specimen UB06 at 166.8 MPa with $\bar{g}=[01\bar{1}]$ contrast in (a), $\bar{g}=[200]$ contrast in (b) and $\bar{g}=[\bar{1}10]$ contrast in (c).

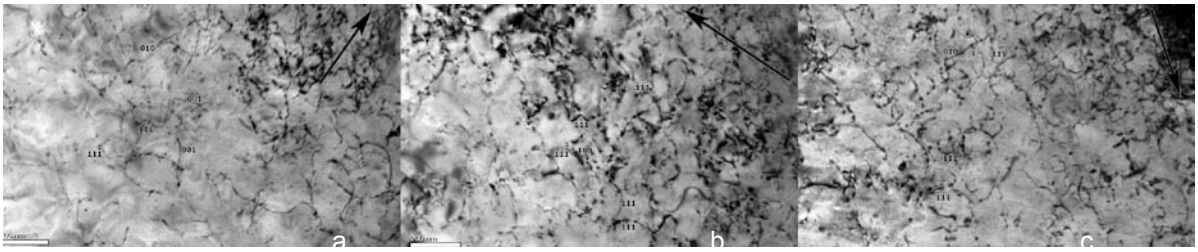

Figure 10. Images of UN19 to identify different Burgers vectors in [01$\bar{1}$] contrast in (a), [200] contrast in (b) and [$\bar{1}$10] contrast in (c), using indices to mark the different Burgers vectors.

Table 2. Truth table for $\bar{g}\bullet\bar{b}$ imaging contrast for the various imaging and Burgers vector conditions used in this study, taken from [4].

Condition	Dislocation Burgers vector						
$\bar{g}$	$\frac{a}{2}$[111]	$\frac{a}{2}$[$\bar{1}$11]	$\frac{a}{2}$[1$\bar{1}$1]	$\frac{a}{2}$[11$\bar{1}$]	a[100]	a[010]	a[001]
[200]	1	1	1	1	2	0	0
[01$\bar{1}$]	0	0	1	1	0	1	1
[$\bar{1}$10]	0	1	1	0	1	1	0
[$\bar{1}$01]	0	1	0	1	1	0	1

Figure 10 is intended to provide insight into the dislocation configurations in V-4Cr-Ti following irradiation at 600ºC. The three contrast conditions have been marked to provide examples of the different Burgers vectors listed in Table 2. For example, a dislocation image marked “100” representing a[100] only appears in $\bar{g}$=[200] imaging but is in strong contrast, whereas a dislocation image marked “111” representing $\frac{a}{2}$[111] only appears in $\bar{g}$=[200] imaging with weaker contrast; a dislocation image marked “11$\bar{1}$” representing $\frac{a}{2}$[11$\bar{1}$] appears in $\bar{g}$=[200] and $\bar{g}$=[01$\bar{1}$] contrast; and so on. Of particular note are dislocation images marked “$\bar{1}$11” representing $\frac{a}{2}$[$\bar{1}$11], one toward the top and the other towards the bottom of the images in Figures 10b) and c). Based on the surface traces that are barely perceptible towards the top of Figure 10b), it is expected that the upper example is in fact a slip dislocation that has moved following specimen preparation. Another example of such behavior can be identified on the right in Figure 1b).

Following the procedure outlined above, dislocation images for the NIFS-Heat2 pressurized tubes were compared and marked as best as possible so that Burgers vectors were determined for each dislocation. This was very difficult in areas containing dislocation tangles at high density. The dislocation densities for each of the seven Burgers vectors present was then determined and results of measurements presented in Table 3. Analysis for the US heat pressurized tube images will be attempted at a later time. Measurements were based on intersections of the dislocation array in an image with a superimposed grid of lines. The grid line length times the thickness represents a surface in the foil so that intersections of a given Burgers vector with that surface divided by the surface area is equivalent to dislocation length per unit volume.

Table 3. Measurements of dislocation density in cm^{-2} for all possible Burgers vectors in the irradiated Japanese pressurized tubes under examination.

Specimen	Dislocation Burgers vector						
	$\frac{a}{2}[111]$	$\frac{a}{2}[\bar{1}11]$	$\frac{a}{2}[1\bar{1}1]$	$\frac{a}{2}[11\bar{1}]$	a[100]	a[010]	a[001]
UN19	3.6×10^8	3.6×10^8	2.7×10^8	2.2×10^8	1.8×10^8	3.1×10^8	3.6×10^8
UN13	4.2×10^8	3.6×10^8	3.1×10^8	8.1×10^8	1.4×10^8	1.6×10^8	2.4×10^8
UN17	5.0×10^8	4.2×10^8	5.9×10^8	6.8×10^8	0.88×10^8	1.5×10^8	1.9×10^8
UN02	6.3×10^8	3.6×10^8	4.0×10^8	5.3×10^8	2.0×10^8	2.0×10^8	2.9×10^8

The results given in Table 3 should probably be considered estimates given the difficulty of the analysis and the time available to perform it. Also, it has not yet been possible to relate the applied stress to the Burgers vector directions. It can be noted from these results that the $\frac{a}{2}$<111> dislocation density for the unstressed condition appears to be lower than that for the stressed conditions, indicating that stress promotes increases in dislocation density. Also, dislocation densities for a<100> Burgers vectors tend to be lower than those for $\frac{a}{2}$<111> Burgers vectors when stress is applied, except for the unstressed case where the a<100> densities are higher. Also, the a<100> dislocation density appears to decrease with increasing stress. However, the results obtained for UN17, the high stress condition, show anisotropy of only about 50% both for $\frac{a}{2}$<111> and a<100> Burgers vectors whereas similar variations are found for UN19, unstressed, and for UN02, at high stress for only about 25% of lifetime.

Discussion

It can be noted that Burgers vectors other than $\frac{a}{2}$<111> have only once been previously identified in V-4Cr-4Ti [9]. This can in part be attributed to the fact that few examinations have been conducted following irradiation at 600ºC, and examinations at lower irradiation temperatures are complicated by extensive oxy-carbo-nitride precipitation. It can be noted that we examined a series of vanadium alloys (excluding V-4Cr-4Ti) following irradiation at 600ºC, and it was concluded that only $\frac{a}{2}$<111> Burgers vectors were found [8]. It therefore may be possible that V-4Cr-4Ti is the exception, but more likely, the effects of precipitation again complicated analysis in that work. Also, it can be noted that our recent post-irradiation work assumed only $\frac{a}{2}$<111> Burgers vectors [10], but interpretation was confusing, probably as a result of the presence of the a<100> Burgers vectors. However, Nakasaka and co-workers recently had the opportunity to examine weldments of the NIFS-HEAT-2 following irradiation at 290ºC to 0.08 dpa in JMTR, and identified black spot damage that did not correspond to an $\frac{a}{2}$<111> Burgers vector [9]. The low irradiation temperature in that experiment was probably not detrimental to imaging because the dose was too low to cause extensive precipitation.

Figure 10 does provide the opportunity to demonstrate that the Burgers vector differing from $\frac{a}{2}$<111> is indeed a<100>. The dislocation marked “001” in Figure 10a) does not appear in Figures 10b) or c). Therefore, the two necessary $\bar{g}\bullet\bar{b}=0$ invisibility criterion are met and the Burgers vector must be a[001]. Considerable discussion has appeared in the literature, trying to explain the observation of a<100> Burgers vectors in ferritic steels, and, in fact, vanadium was predicted to have a higher probability for a<100> loop formation than was ferritic steel, 5.5×10^{-5} versus 5.7×10^{-9} [11]. Those probability predictions ranked niobium slightly higher than vanadium and tungsten much lower, at 1.4×10^{-27}.

The dislocation configurations found in unstressed and stressed V-4Cr-4Ti irradiated pressurized tubes can be summarized as follows. After irradiation at 600ºC to 3.7 dpa in HFIR, a dislocation network develops that includes $\frac{a}{2}$<111> and a<100> burgers vectors. The complex network is difficult to envision unless all dislocation line segments in a field of view can be understood; individual line segments often appear in individual images. Therefore, the network can be defined by the dislocation nodes or points where line segments meet. However, many examples can be shown both for stressed and unstressed samples where

the line segments are bowed into arcs, indicating that considerable stress develops during irradiation by the preferential absorption of interstitials, and the nodes restrain the dislocation motion.

Application of stress is expected to preferentially influence those Burgers vectors that are favorably oriented with respect to the stress axis. This is the case both during loop nucleation and dislocation climb. As a consequence, those Burgers vectors favorably oriented are expected to develop high populations and densities, and this study was intended to quantify that behavior in V-4Cr-4Ti. The procedure has been hindered by the observation that dislocations are found to slip in the foil either during preparation, loading or examination, changing the apparent populations. However, it was a relatively simple matter to restrict quantification to areas where no apparent slip had occurred.

As the Burgers vector anisotropy develops, it is expected that the anisotropy will continue to increase unless there is a process restraining it. This is because any favored Burgers vector is expected to climb more rapidly than an unfavored Burgers vector as predicted by SIPA, resulting in even more line length and further increases in anisotropy. The restraining process is likely to be a result of the internal stress that results from the presence of the anisotropy. The sum of all dislocation stress fields will produce an internal stress state, the larger the anisotropy, the larger the non-hydrostatic portion of the internal stress state. It is anticipated that the internal stress state will increase until it matches the externally applied stress, and then the Burgers vector anisotropy will stabilize, reaching a steady state.

However, the present attempt to measure the consequences of irradiation creep as Burgers vector anisotropy is not definitive. Anisotropy measurements for the high stress condition were similar to those at lower stress. Comparison with previous results show that for ferritic steels,[4] anisotropies for samples at hoop stresses of 86 and 60 MPa irradiated at 420ºC produced higher dislocations densities and higher anisotropies, on the order of a factor of 7 variation for $\frac{a}{2}$<111> Burgers vectors and 3 to 5 for a<100> Burgers vectors. Also, the densities for a<100> Burgers vectors were comparable to those for $\frac{a}{2}$<111>. Our results are surprising because the anisotropy found was small compared to those other materials. However, the creep coefficient measured at 600ºC for the US heat heat of V-4Cr-4Ti was 5×10^{-6} $MPa^{-1}dpa^{-1}$, compared to ~0.5 $\times 10^{-6}$ $MPa^{-1}dpa^{-1}$ for ferritic/Martensitic steels and ~1 $\times 10^{-6}$ $MPa^{-1}dpa^{-1}$ for austenitic stainless steels [7]. The consequences are not yet understood.

When a pressurized tube fails, it can be anticipated that the anisotropic Burgers vector populations will continue to evolve for some time before the anisotropy dissipates. To study this response, images were collected for specimen UN02. Based on the diameter change for UN02 in comparison with UN17, it is likely that UN02 failed after about 27% of goal fluence. Therefore, anisotropy measurements in UN02 will give insight into the dose needed to return the dislocation structure to an isotropic condition. Given the observation that the dislocation structure is a network defined by nodes, returning the structure to an isotropic condition can be envisioned as a process that simply shifts the nodal positions, and therefore isotropy could be reached quickly. Interestingly, the anisotropy observed in UN02 is similar to UN17 suggesting that an isotropic condition was not attained, but it should also be also noted that the same level of anisotropy is present in all of the specimens examined regardless of applied stress.

Conclusions

Seven V-4Cr-4Ti pressurized tubes from the HIFR 17J irradiation experiment, three of US heat 832665 and four of heat NIFS-heat2, have been examined by transmission electron microscopy in order to measure Burgers vector anisotropy produced during irradiation creep and subsequent growth after tube failure. It was found that both materials developed precipitation in reactor at 600ºC, the US heat probably containing TiO_2 and the Japanese heat forming oxy-carbo-nitrides, but precipitation did not prevent satisfactory dislocation imaging. Also, it was found that V-4Cr-4Ti develops both $\frac{a}{2}$<111> and a<100> Burgers vectors during irradiation, with the a<100> dislocation densities similar to those with $\frac{a}{2}$<111> for an unstressed condition but lower as a result of applied stress. However, Burgers vector anisotropy measurements in V-4Cr-4Ti did not show the large variations found in ferritic steels.

Future Work

Anisotropy measurements will be continued and it is hoped that this work will shift to modeling Burgers vector anisotropy in order to estimate the internal stress state generated by Burgers vector anisotropy and to dislocation interactions during post-irradiation deformation. Also, issues will be considered regarding growth response when stresses relax.

References

[1] E. Orowan in Proceedings, Physical Society, Vol. 52 (1940) 8.

[2] D. S. Gelles, F. A. Garner and H. R. Brager, in Proc. ASTM Tenth International Symposium on Effects of Radiation on Materials, Savannah, GA, June 1980, p. 735.

[3] D. S. Gelles, in Proc. ASTM Twelfth International Symposium on Effects of Radiation on Materials, Williamsburg, VA, 1984, ASTM STP 870, p. 98-112.

[4] D. S. Gelles, A. Kimura and T. Shibayama, in Effects of Radiation on Materials: 19th International Symposium, ASTM STP 1366, M. L. Hamilton, A. S. Kumar, S. T. Rosinski, and M. L. Grossbeck, Eds., American Society for Testing and Materials (2000) 535.

[5] D. S. Gelles, DOE/ER-0313/29 (2001) 45.

[6] K. Fukumoto, M. Narui, H. Matsui, T. Nagasaka, T. Muroga, M. Li, D. Hoelzer and S. J. Zinkle, J. Nucl. Mater., 386-388 (2009) 575.

[7] M. Li, D. T. Hoelzer, M. L. Grossbeck, A. F. Rowcliffe, S. J. Zinkle and R. J. Kurtz, J. Nucl. Mater., 386-388 (2009) 618, and M. Li, ANL, private communication.

[8] D. S. Gelles and J. F. Stubbins, J. Nucl. Mater. V212-215 (1994) 778, or DOE/ER-0313/15 (1994) 115.

[9] T. Nagasaka, T. Muroga, H. Watanabe, K. Yamasaki, N. J. Heo, K. Shinozaki and M. Narui, Mater. Trans. Japan Inst. Metals, 46 (2005) 498-502.

[10] D. S. Gelles, M. B. Toloczko and R. J. Kurtz, DOE/ER-0313/47 (2010) 1.

[11] E. A. Little, R. Bullough, and M. H. Wood, Proc. R. Soc. Lond. A372 (1980) 565.